

# Effect of Cold Isostatic Pressing and VC Grain Growth Inhibitor Addition on WC Grain Size and Mechanical Properties of WC-8Co Cemented Carbide

Gennadiy Akimov

*Donetsk Institute for Physics and Engineering named after O.O. Galkin  
of the National Academy of Sciences of Ukraine, Kyiv, UKRAINE*

Ihor Andreev, Tamara Kosenchuk

*V. Bakul Institute for Superhard Materials of the National Academy of  
Sciences of Ukraine, Kyiv, UKRAINE*

Vitalii Sheremet\*, Iryna Trosnikova, Petro Loboda

*National Technical University of Ukraine ,  
“Igor Sikorsky Kyiv Polytechnic Institute”, Kyiv, UKRAINE  
\*v.sheremet@kpi.ua*

## ABSTRACT

*In this study, sub-micron WC-Co cemented carbides were fabricated by cold isostatic pressing using recycled WC powder, Co powder, and VC grain growth inhibitor as the initial composite powders. The raw WC-8Co and WC-8Co-0.3VC compositions were prepared according to conventional technology. After that, part of the green compacts was CIP-ed under pressure of 200 MPa. Sintering was carried out in an industrial vacuum sintering furnace at a temperature of 1420 °C simultaneously for all samples. The microstructures and properties, including density, coercivity, transverse rupture strength, A-type Rockwell hardness and fracture toughness were investigated, characterized and compared systematically. The experimental results showed that the action of cold isostatic pressing in combination with grain growth inhibitor addition promoted ultrafine grains with the finest WC grain size of 0.68  $\mu\text{m}$  and an increase in the fracture toughness up to 15.4  $\text{MPa}\cdot\text{m}^{1/2} \pm 0.2$  compared to rest cemented carbides, showing the technique*

*has potential to fabricate cermets with both small average WC grain size and high fracture toughness, which is key in providing excellent performance.*

**Keywords:** *Cold Isostatic Pressing; Coercivity; WC Grain Size; Grain Growth Inhibitor; Transverse Rupture Strength*

## Introduction

Cemented carbides are one of the most used powder metallurgy products worldwide. Due to their superb combination of wear resistance and strength compared to other cutting materials, such as diamond or high-speed steels, these materials gained more popularity. This is possible due to the combination of superhard tungsten carbide and more ductile cobalt in the composite. Over the past few decades, intensive research efforts have been devoted to reducing the grain size of WC. One of the first systematic studies of the effect of grain growth inhibitor (GGI) on the microstructure and properties of cemented carbides was by Schwarzkopf et al. [1], followed by a considerable amount of works [2]-[8].

Among all grain growth inhibitors, VC and Cr<sub>3</sub>C<sub>2</sub> are the most frequently used [3]. Currently, the mechanism of interaction of (W, V)C<sub>x</sub> complexion at the WC/Co interface has not been yet sufficiently understood [3]. Taken together, studies [2]-[8] provide evidence that the use of 0.2-0.4 wt.% VC GGI addition in WC-Co cemented carbides exhibits a reduced mean WC grain size. However, the addition of VC GGI decreases the fracture toughness and strength [2]-[3] due to the presence of (W, V)C<sub>x</sub> complexion at the interface between Co and WC. The fraction of the interface coherency of the VC addition is only 8% that for Cr<sub>3</sub>C<sub>2</sub> is 18% and in the case without GGI addition is up to 21% [3]. Such incoherence weakens the interface material and consequently reduces the strength of WC-Co cemented carbides. Also, due to a decrease in the cobalt mean free path of GGI-containing carbides, the plasticity resource of the binder is exhausted earlier [9].

Hardness and fracture toughness are vital properties for ensuring high performance of cemented carbides. By making changes to the WC grain size and the coherency of the WC/Co interface, it is possible to determine the above-mentioned properties of the cemented carbides [4]. Hardness is known to increase as the WC grain size decreases. Alloys containing GGI additives show higher hardness due to finer WC grains compared to GGI-free cemented carbides. However, the fracture toughness exhibits an inverse tendency and decreases with decreased Co mean free path [10]. Moreover, the role of the Co binder on fracture toughness becomes less important with a decreased in Co mean free path [9] due to the increased role of the coherency of the WC/Co interface and the phase transformation of cobalt [11]. Currently, there are

almost no studies showing a satisfactory combination of high strength, hardness, and fracture toughness would be obtained.

In a recent study [12] which set out to determine the effect of cold isostatic pressing (CIP) on the properties of WC-8Co cemented carbide, it was shown that the CIP of samples before sintering was accompanied by a significant reduction in mean WC grain size compared to unCIP-ed samples.

This study explored the combined effect of preliminary CIP of green bodies and VC GGI addition on the mean WC grain size and mechanical properties of sintered bulk samples.

## **Experimental**

Recycled tungsten carbide powder (WC agglomerates,  $F_{88} = \sim 10 \mu\text{m}$ , quality assurance according to the TU 48-19-72-92, Development and application of new materials Ltd., Ukraine), commercial cobalt (98 wt.% Co), and VC powder (99 wt.% VC) were used as initial materials. The compositions of the experimental cemented carbides were WC-8Co (wt.%) and WC-8Co-0.3VC (wt.%). These compositions correspond to the domestic grades of cemented carbides, namely “VK8” and “VK8M”, which are widely used for cutting in difficult conditions. To obtain uniform mixtures, the raw powder compositions were separately ball-milled in the milling vial with 12 mm cemented carbide balls using ethyl alcohol as a milling medium for 40 hours. After milling, the powders were dried. To ensure good formability of the raw material, the powder composition was mixed with a plasticizer. As a formative agent, a 5% solution of synthetic rubber in gasoline was used at the ratio of 0.15 L of the solution per 1 kg of the mixture. The optimal ratio of the formative agent to the powder was chosen according to the technological instruction 25000.20072 “mixing carbide compositions”.

After uniaxial pressing in a steel die under a pressure of 70 MPa, the samples were dried at 120 °C for 24 hours. The green bodies of WC-8Co-0.3VC composition were divided into two groups. Subsequently, one was put into an elastic mold and densified by CIP at 200 MPa. The CIP was carried out on multiplication high-pressure equipment PMM-125 (Ministry of Instrument-Making, Automation Devices and Control Systems, USSR). Sintering of all samples was carried out in an industrial vacuum sintering furnace at 1440 °C. Samples were prepared for microstructural analysis and mechanical properties measurement by grinding and polishing.

The bulk density of the sintered alloys was measured according to Archimedes principle. The coercivity was measured with a Cobalt-1 (Elektrotochpribor BY “Volna”, Chisinau, Moldova) coercivity meter. The TRS was measured using a three-point bend test according to the ASTM B406 standard with a loading rate of 2 mm/min. Scanning electron microscope (SEM) REM-106I (Selmi Ltd., Sumy, Ukraine) was used to identify the size

of the WC particles. The microstructure was studied using an Axia ChemiSEM HiVac (Thermo Fisher Scientific Brno Ltd., Brno, Czech Republic) SEM. The mean WC grain size of the sintered samples was measured by image analysis using JMicrovision software [13]. To ensure statistical representation, at least 600 WC grains were measured by semi-automatic method [14] based on SEM images were used to obtain the size distribution and the average size of WC grains. The hardness of the specimens was measured by an A-type Rockwell hardness tester using a ZIP TK-2 indenter with a loading of 60 kg. The  $K_{IC}$  was determined by measuring the cracks from the Vickers indentation using a 50 kg load and then calculating according to the Palmqvist equation [15] Equation (1):

$$K_{IC}=0.0028 (H_V P/L)^{1/2} \quad (1)$$

where  $H_V$  is the Vickers indentation hardness,  $P$  is the indentation load, and  $L$  is the total crack length.

## Results and Discussion

### Microstructure

Figure 1a is an image of the initial WC-8Co powder composition and Figure 1b shows the statistical WC particle size distribution. The mean particle size of the as-milled WC powder used in this work was 0.63  $\mu\text{m}$ .

The WC powder particles are homogeneously distributed in a range of 0.4-0.6  $\mu\text{m}$  Figure 1b. The image analysis indicated that about 10% of the particles were in the range of 1.0-1.6  $\mu\text{m}$ , which in terms of volume fraction is about 40%. Different sintering behaviors are observed for particles of different sizes. During liquid-phase sintering, the smallest WC particles are dissolved first. Thus, a significant volume of particles in the range of 1.0-1.6  $\mu\text{m}$  plays a less important role during sintering than the largest ones. However, the high isostatic pressure of CIP primarily acts on the largest particles, possibly destroying them and preliminarily mechanically activating their surfaces, these mechanisms are described in detail elsewhere [12]. By making changes to the sintering processes, CIP significantly reduced the WC grain size in the sintered alloy. The average WC grain size, the Co mean free path and the coercivity of the WC-8Co and WC-8Co-0.3VC are listed in Table 1.

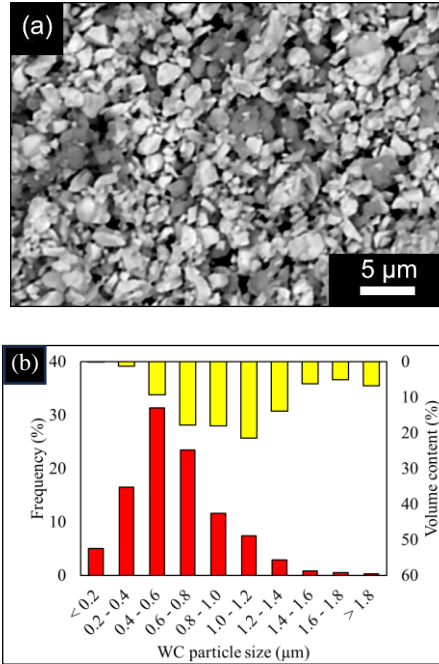


Figure 1: SEM image of the morphology (a) and the statistical WC particle size distribution, and (b) of the initial powder composition

Table 1: Comparison of the WC average grain size, the Co mean free path and the coercivity of WC-8Co and WC-8Co-0.3VC cemented carbides

Samples	WC grain size (μm)	Co mean free path (μm)	Coercivity (kA/m)
WC-8Co	0.88	0.20	13.0 ± 0.26
WC-8Co-0.3VC	0.80	0.15	14.4 ± 0.29
WC-8Co-0.3VC CIP-ed	0.68	0.11	19.7 ± 0.39

The Co mean free path decreased with decreased WC grain size. Table 1 also lists the value of coercivity which increased from 13.0 kA/m ± 0.26 to 19.7 kA/m ± 0.39, implying the inversely proportional relationship between grain size and coercivity [16]. The effect of the VC GGI addition was enhanced by the pre-CIP of samples. The WC grain size distribution in Figure 2 shows the CIP-ed samples had the finest WC grain structure. The mean WC grain size of the WC-8Co-0.3VC alloy was about 0.80 μm. After applying CIP, that for the same alloy was decreased to 0.68 μm.

Figure 3 compares the SEM surface structures of sintered alloys. Hardness and TRS are the most important properties of cemented carbides. As

is well known, the hardness of cemented carbides is a function of the WC grain size according to the Hall-Petch relationship [17]. The shape of the WC grains was also different. In WC-8Co and WC-8Co-0.3VC alloys, the WC grains were mostly angular, while in WC-8Co-0.3VC CIP-ed alloys, the WC grains were more rounded. The equilibrium shape of WC crystals is dictated by its surface energy anisotropy [18]. The results, as shown in Table 2, indicate that the hardness increased slightly as the WC grain size decreased.

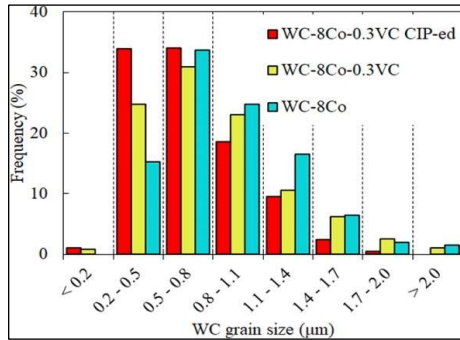


Figure 2: WC grain size distribution of WC-8Co, WC-8Co-0.3VC and WC-8Co-0.3VC CIP-ed cemented carbides

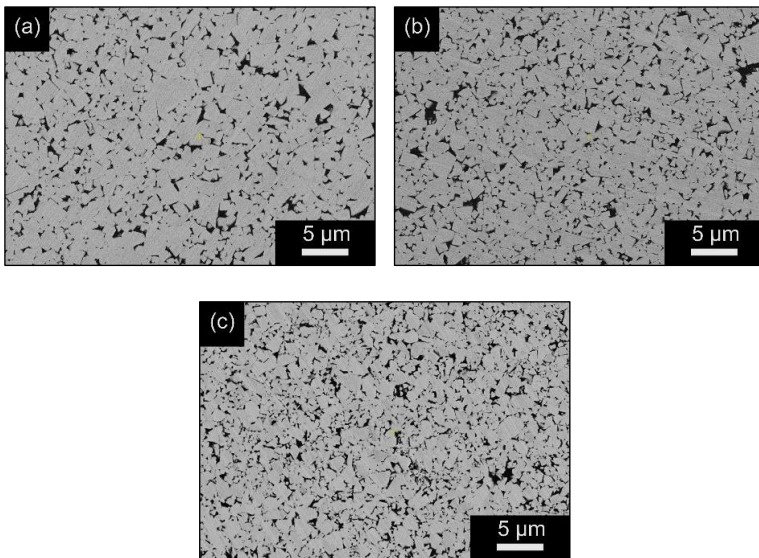


Figure 3: SEM images of the surface of sintered alloys: (a) WC-8Co, (b) WC-8Co-0.3VC, and (c) WC-8Co-0.3VC CIP-ed

However, the TRS results indicated that both alloys with VC addition had the lowest TRS values ( $1030 \pm 97$  and  $1200 \pm 83$  MPa for CIP-ed and unCIP-ed samples, respectively). Conversely, the TRS of GGI-free alloy reached  $1650 \pm 65$  MPa

Table 2: Density, Rockwell hardness and TRS of WC-8Co and WC-8Co-0.3VC cemented carbides

Samples	Density (g/cm <sup>3</sup> )	HRA	TRS (MPa)	K <sub>1C</sub> (MPa m <sup>1/2</sup> )
WC-8Co	14.8	90.00 ± 0.30	1650 ± 65	12.0 ± 0.3
WC-8Co-0.3VC	14.8	90.25 ± 0.30	1200 ± 83	10.1 ± 0.2
WC-8Co-0.3VC CIP-ed	14.6	90.30 ± 0.30	1030 ± 97	15.4 ± 0.2

The density of the sintered cemented carbides is also listed in Table 2, and the results show that the density of each presented sample was close to the theoretical value.

### **Effect of CIP on WC-8Co-0.3VC cemented carbide**

Previously [19], various CIP pressures up to 400 MPa were examined in order to determine the optimal one, as well as to compare the properties of cemented carbides. Samples that underwent preliminary CIP at 200 MPa showed maximum density and minimum WC grain size after sintering. Cold isostatic pressing is useful to obtain a uniform distribution of density over the entire volume of the workpiece due to isostatic application of pressure and the absence of die-wall frictional forces. CIP ensures homogeneous compaction of the green body and, as a result, promotes uniform shrinkage during sintering and isotropy of the physical and mechanical properties of the ceramic products [20]. During CIP, compaction occurs primarily due to the sliding of powder particles relative to each other, which takes place under conditions of their quasi-isostatic compression [21] by other WC and Co particles; at this stage, an arched structure of the largest and relatively large particles appears. With increasing CIP pressure, unstable arch structures are formed and then destroyed again and again when peak stress is reached on the elements of the arch structure - WC grains. Obviously, the cycles of formation and destruction are accompanied by the compaction of the green body. Previous research [12] established that the largest WC particles can be crushed with increasing CIP pressure.

The eutectic is probably formed mainly from the mechanically activated fragments of large particles destroyed during CIP. Thus, fragments of large particles either partially or completely dissolve, resulting in WC grain refinement. A systematic literature review concluded that for a given alloy composition at the eutectic formation temperature (1320 °C), up to 8 wt.% of

WC dissolves in Co. Furthermore, an increase in the sintering temperature up to 1440 °C was followed by the usual processes [19]. In addition, according to the above-mentioned results, the smaller WC grain sizes are the major factor that leads to a decrease in the Co mean free path. Comparing the results, in the cemented carbides prepared by using CIP treatment of green bodies, the mean WC grain size is much finer than that of the unCIP-ed cemented carbides. The most obvious finding to emerge from the analysis is that the conditions leading to a decrease in the WC grain size are formed before sintering during CIP. In addition, during liquid-phase sintering, the effects of CIP mechanical activation of the green WC-8Co-0.3VC bodies and the action of VC GGI addition, the mechanism of which is described in the introduction, are combined.

### **Transverse Rupture Strength (TRS)**

In general, analyzing the combined effect of CIP and VC GGI addition on the coercivity, the magnetic properties of hard alloys are determined by the content and morphology of the Co metal binder [16]. Adding VC GGI in the WC-8Co composition and the use of 0.2 GPa CIP increased the coercivity and significantly decreased the WC grain size, hence, leading to an increase in the specific surface area of WC grains and a decrease in the thickness of the Co layer. Thus, for the first time, it was found that the combined action of VC addition and CIP leads to ultrafine microstructure. However, the TRS value depends strongly on the Co distribution and the state of the interface layer between the Co binder and WC grains. Figure 4 shows the TRS fracture surface of WC-8Co and WC-8Co-0.3VC cemented carbides.

Figure 4 shows clearly that the use of CIP caused a significant change in the microstructure of the alloy. Significant changes in the microstructure of the alloy affected the strength. It is well established, that the crack in cemented carbides is developed intercrystalline between WC grains and Co binder phase [22]. Cobalt is characterized by significant dislocation plasticity, while the plasticity of WC is insignificant [23]. The Co plastic deformation is inhibited due to the strain-hardening (SH) [24]. It is also well established that the Co binder of WC-Co cemented carbides undergoes a phase transformation from unstable FCC to HCP during plastic deformation, inhibiting dislocation movement due to the limited number of slip systems in HCP crystal structure [25]. Hence, the intense crack propagation is attributed to the SH effect of the Co binder phase with increasing load. It is shown that the TRS decreases with decreasing the WC grain size, due to the thinning of the thickness of the cobalt layer and the exhaustion of the plasticity limit during SH. Also, a newly formed  $(W_xV_y)C$  solid solution phase plays a negative role in the formation of the TRS value, due to the VC GGI addition. The fraction of interface coherency in the case of VC GGI addition is very low (about 8%) [3]. The incoherence makes the interface weaker, and the failure crack

propagates through the interface therefore this is the reason for the decrease in the strength of VC-doped alloys observed in this work.

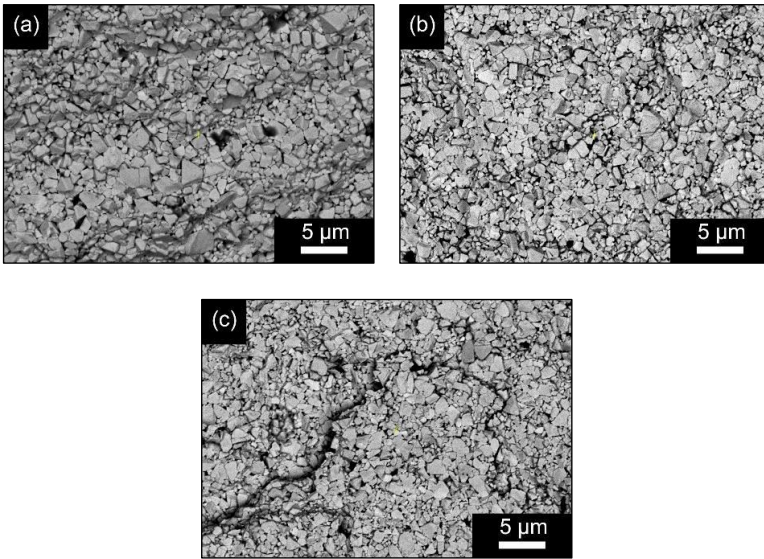


Figure 4: SEM images showing fracture surfaces of sintered alloys: (a) WC-8Co, (b) WC-8Co-0.3VC, and (c) WC-8Co-0.3VC CIP-ed

### **Fracture toughness**

The mechanism of interaction between  $(W, V)C_x$  complexion at the WC/Co boundary has not been sufficiently understood yet. Cemented carbides without GGI have the highest fraction of the interface coherency. Cemented carbide with VC GGI addition has almost 3 times lower fraction of the WC/Co interface coherency than that of the alloy without GGI due to the presence of high stability  $(W, V)C_x$  complexion [3]. Such a difference affected the fracture toughness of the cemented carbide give up a significant decrease in the ability to resist against the intergranular fracture. It has also been reliably established that the presence of complexion at the WC/WC interface improves the fracture toughness of WC-Co cemented carbides due to a decrease in the contiguity of WC grains [26]. However, the crack does not always propagate along the interface where the complexion exists due to the discontinuous distribution of the  $(W, V)C_x$  complexion [3] as marked in Figure 5.

As reported in recent publications [12], [19] and which is consistent with the data obtained in this work CIP-ed samples have finer WC grain size compared to those that did not pass CIP. This implies that the Co mean free path in CIP-ed samples was decreased which was accompanied by a rapid increase in specific surface area of WC grains. Perhaps, there was a limitation

associated with a lack of V for the formation of the  $(W, V)C_x$  complex on the entire surface of the WC/Co interface. Based on the findings of studies on the influence of VC in the formation of a complex at the WC/Co boundary [3], [6], it is likely that the areas free of complex appear in Figure 5. From the results, it can be seen that such a change in the size of WC grains can change the proportion of the cracks along the interface and affect the fraction of the WC/Co interface coherency. The results confirm that CIP dramatically increased the fracture toughness of the cemented carbide.

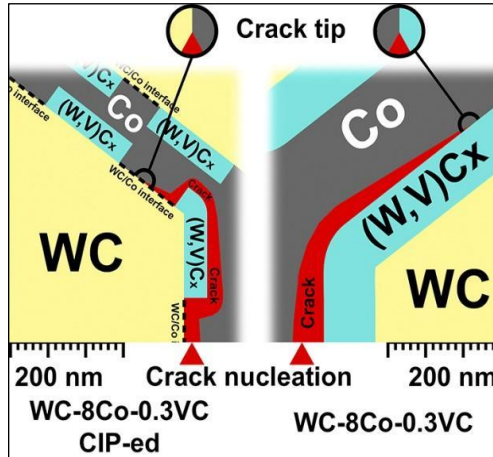


Figure 5: Schematic diagram of Palmquist crack propagation in WC-8Co-0.3VC and WC-8Co-0.3VC CIP-ed cemented carbides

## Conclusions

Thus, for the first time, it was shown that the action of CIP in combination with the VC addition leads to an ultrafine microstructure. In the WC-8Co-0.3VC CIP-ed samples a large fraction of WC grains was in the range of 0.2-0.8  $\mu\text{m}$ , with a mean WC grain size of about 0.68  $\mu\text{m}$ . By contrast, coarser WC grains with the size of 0.80  $\mu\text{m}$  and 0.88  $\mu\text{m}$  were found for the alloys WC-8Co-0.3VC and WC-8Co. The fracture toughness of the cemented carbides increased due to the smallest grain size in CIP-ed samples, which influenced the fraction of the WC/Co interface coherency. The WC-8Co-0.3VC CIP-ed alloy had a fracture toughness of  $15.4 \text{ MPa}\cdot\text{m}^{1/2} \pm 0.2$ , whereas the fracture toughness of the WC-8Co-0.3VC unCIP-ed alloy was only  $10.1 \text{ MPa}\cdot\text{m}^{1/2} \pm 0.2$ .

## **Contributions of Authors**

The authors confirm the equal contribution in each part of this work. All authors reviewed and approved the final version of this work.

## **Funding**

This work received no specific grant from any funding agency.

## **Conflict of Interests**

All authors declare that they have no conflicts of interest.

## **Acknowledgment**

The authors are indebted to Prof. O. Kolot for his help in creating the cold isostatic pressing machine for the experiments. The authors would also like to thank to PhD student S. Teslia and Senior researcher Yu. Romanenko (National Technical University of Ukraine “Igor Sikorsky Kyiv Polytechnic Institute”) for their technical support in SEM characterization.

## **References**

- [1] P. Schwarzkopf and R. Kieffer, *Cemented carbides*. 1960.
- [2] X. Li, L. Wang, Y. Liu, and J. Ye, “Enhanced high temperature mechanical properties of WC-Co cemented carbides by VC addition,” *International Journal of Refractory Metals and Hard Materials*, vol. 116, p. 106355, 2023, doi: 10.1016/j.ijrmhm.2023.106355.
- [3] X. Liu, X. Song, H. Wang, X. Liu, F. Tang, and H. Lu, “Complexions in WC-Co cemented carbides,” *Acta Materialia*, vol. 149, pp. 164–178, 2018, doi: 10.1016/j.actamat.2018.02.018.
- [4] S. Budin, K. M. Hyie, and M. A. Selamat, “The effect of adding carbon and vanadium carbide on microstructure and mechanical properties of ultra-fine WC-Co composite,” *Journal of Mechanical Engineering*, vol. 5, no. 4, pp. 25–36, 2018.
- [5] B. Wang, Z. Wang, Z. Yin, J. Jua, and J. Jia, “Preparation and properties of the VC/Cr<sub>3</sub>C<sub>2</sub>/TaC doped ultrafine WC-Co tool material by spark plasma sintering,” *Journal of Alloys and Compounds*, vol. 816, no. 2, pp. 1–30, 2020, doi: 10.1016/j.jallcom.2019.152598.

- [6] W. Y. Ning, N. Muhamad, A. B. Sulong, A. Fayyaz, and M. R. Raza, "Effects of vanadium carbide on sintered WC-10%Co produced by micro-powder injection molding," *Sains Malaysiana*, vol. 44, no. 8, pp. 1175–1181, 2015, doi: 10.17576/jsm-2015-4408-14.
- [7] F. Arenas, I. Arenas, J. Ochoa, and S.-A. Cho, "Influence of VC on the microstructure and mechanical properties of WC-Co sintered cemented carbides," *International Journal of Refractory Metals and Hard Materials*, vol. 17, nos. 1–3, pp. 91–97, 1999, doi: 10.1016/s0263-4368(98)00061-4.
- [8] C. Yin, Yingbiao Peng, J. Ruan, Lin Zhao, Renhe Zhang, and Yong Du, "Influence of Cr<sub>3</sub>C<sub>2</sub> and vc content on wc grain size, wc shape and mechanical properties of WC-6.0 wt.% Co cemented carbides," *Materials*, vol. 14, no. 6, p. 1551, 2021, doi: 10.3390/ma14061551.
- [9] X. Song, Y. Gao, X. Liu, C. Wei, H. Wang, and W. Xu, "Effect of interfacial characteristics on toughness of nanocrystalline cemented carbides," *Acta Materialia*, vol. 61, no. 6, pp. 2154–2162, 2013, doi: 10.1016/j.actamat.2012.12.036.
- [10] X. Xu *et al.*, "Preparation of highly toughened Ti(C,N)-based cermets via mechanical activation and subsequent in situ carbothermal reduction," *International Journal of Refractory Metals and Hard Materials*, vol. 92, pp. 1–5, 2020, doi: 10.1016/j.jirmhm.2020.105310.
- [11] V.K. Sarin and T. Johannesson, "On the deformation of WC-Co cemented carbides," *Metal Science*, vol. 9, pp. 472–476, 1975, doi: 10.1179/030634575790444531.
- [12] G. Ya. Akimov, I. V. Andreev, V. I. Sheremet, I. Yu. Trosnikova, P. I. Loboda, and T. O. Kosenchuk, "The structure and mechanical properties of WC-8 wt.% Co hardmetal produced by cold and hot isostatic pressing," *Powder Metallurgy and Metal Ceramics*, vol. 61, no. 1–2, pp. 9–17, 2022, doi: 10.1007/s11106-022-00290-0.
- [13] "Download - JMicroVision," *jmicrovision.github.io*. [Online]. Available: <https://jmicrovision.github.io/download.htm> (Accessed Mar. 29, 2024).
- [14] M. Brieseck, W. Lengauer, B. Gneiß, K. Wagner, and S. Wagner, "A straightforward method for analysing the grain-size distribution in tungsten carbide - cobalt hardmetals," *Microchimica Acta*, vol. 168, no. 3–4, pp. 309–316, 2010, doi: 10.1007/s00604-010-0294-4.
- [15] D. W. Trindade, R. da Silva Guimarães, R. D. Lugon, E. R. Gonçalves Junior, A. A. A. dos Santos, and M. Filgueira, "Experimental study to assess fracture toughness in SPS sintered WC-10% Co hardmetal by modifying the palmqvist test," *Coatings*, vol. 12, no. 12, pp. 1–16, 2022, doi: 10.3390/coatings12121809.
- [16] D. Mueller, I. Konyashin, S. Farag, and B. Ries, "A novel express method for determining WC grain sizes and its use for updating dependencies of coercivity and hardness on WC mean grain size in hardmetals,"

- International Journal of Refractory Metals and Hard Materials*, vol. 117, p. 106416, 2023, doi: 10.1016/j.ijrmhm.2023.106416.
- [17] N. Hansen, “Hall–Petch relation and boundary strengthening”, *Scripta Materialia*, vol. 51, no. 8, pp. 801–806, 2004, doi: 10.1016/j.scriptamat.2004.06.002.
- [18] Z. Fang, P. Maheshwari, X. Wang, H.Y. Sohn, A. Griffo, and R. Riley, “An experimental study of the sintering of nanocrystalline WC-Co powders,” *International Journal of Refractory Metals and Hard Materials*, vol. 23, no. 4–6, pp. 249–257, 2005, doi: 10.1016/j.ijrmhm.2005.04.014.
- [19] G. Ya. Akimov *et al.*, “The effect of cold isostatic pressing of powder billets produced from the VK8 hardmetal on its hardness and phase composition after sintering,” *Powder Metallurgy and Metal Ceramics*, vol. 60, no. 3–4, pp. 142–149, 2021, doi: 10.1007/s11106-021-00235-z.
- [20] J. García, V. C. Ciprés, A. Blomqvist, and B. Kaplan, “Cemented carbide microstructures: a review,” *International Journal of Refractory Metals and Hard Materials*, vol. 80, pp. 40–68, 2019, doi: 10.1016/j.ijrmhm.2018.12.004.
- [21] G. Ya. Akimov, I. Yu. Prokhorov, and V. M. Timchenko, “Effect of quasi-hydrostatic compression on the mechanical properties of ceramics in the  $ZrO_2 + 3 \text{ MOL.}\% \text{ Y}_2O_3$  System,” *Refractories and Industrial Ceramics*, vol. 43, no. 3/4, pp. 100–102, 2002, doi: 10.1023/a:1019651027479.
- [22] F. De Luca *et al.*, “Nanomechanical Behaviour of Individual Phases in WC-Co Cemented Carbides, from Ambient to High Temperature.,” *Materialia*, vol. 12, p. 100713, 2020, doi: 10.1016/j.mtla.2020.100713.
- [23] V. Tong, H. Jones, and K. Mingard, “Micropillar compression of single crystal tungsten carbide, part 2: Lattice rotation axis to identify deformation slip mechanisms,” *International Journal of Refractory Metals and Hard Materials*, vol. 103, p. 105734, 2022, doi: 10.1016/j.ijrmhm.2021.105734.
- [24] I. Bogomol and P. Loboda, “Directionally Solidified Ceramic Eutectics for High-Temperature Applications,” *IGI Global eBooks*, pp. 303–322, 2013, doi: 10.4018/978-1-4666-4066-5.ch010.
- [25] V. K. Sarin and T. Johansson, “On the deformation of WC–Co cemented carbides,” *Metal Science*, vol. 9, pp. 472–476, 1975, doi: 10.1179/030634575790444531.
- [26] M. Padmakumar and D. Dinakaran, “A review on cryogenic treatment of tungsten carbide (WC-Co) tool material,” *Materials and Manufacturing Processes*, vol. 36, pp. 637–659, 2021, doi: 10.1080/10426914.2020.1843668.